Advances in Materials Research, *Vol. 10*, *No. 1* (*2021*) *57-66*
DOI: https://doi.org/10.12989/amr.2021.10.1.057

Forced vibration analysis of a fiber reinforced composite beam

Ş.D. Akbaş*

Department of Civil Engineering, Bursa Technical University, 16330, Bursa, Turkey

(*Received August 27, 2020, Revised January 3, 2021, Accepted January 19, 2021*)

Abstract. In this study, forced vibration analysis of a fiber reinforced composite cantilever beam is investigated under a harmonic load. In the beam model, the Timoshenko beam theory is used. The governing equations of problem are derived by using the Lagrange procedure. In the solution of the problem the Ritz method is used and algebraic polynomials are used with the trivial functions for the Ritz method. In the solution of the forced vibration problem, the Newmark average acceleration method is used in the time history. In the numerical examples, the effects of fibre orientation angles, the volume fraction and dynamic parameters on the forced vibration response of fiber reinforced composite beam are presented and discussed.

Keywords: fiber reinforced composite materials; forced vibration analysis; Timoshenko Beams; Ritz Method

1. Introduction

Fiber reinforced composite structures mainly preferred in the engineering projects due to their higher strength-weight ratios, more lightweight and ductile properties. The dynamic effects are very important for design of FRC structures because their slender geometry.

Some investigations about dynamic analysis of FRC structures are as follows; Krawczuk *et al.* (1997) studied the vibration of cracked composite beams. Palanivel (2006) performed the free vibration analysis of laminated composite beams by using two high-order shear deformation theory and finite elements method. DeValve and Pitchumani (2014) investigated damping vibration analysis of rotating composite beams with embedded carbon nanotubes. Tornabene *et al.* (2014) investigated static and vibration analysis of laminated doubly-curved shells and panels embedded in elastic foundation by using the generalized differential quadrature. Pour *et al.* (2015) presented nonlinear vibration of single walled carbon nanotubes by using differential quadratic method. Mohanty *et al.* (2015) investigated dynamic responses of functionally graded pre-twisted beams by using Timoshenko beam theory and finite element method. Akbaş (2014a, c) presented wave propagation of cracked beams under impact loads. Akbaş (2014b, 2015b, 2018a, c, 2019a, c, 2021) investigated dynamic analysis of functionally graded composite beams with different dynamic cases. Ebrahimi *et al.* (2016), Ebrahimi and Barati (2017) investigated dynamic responses of inhomogeneous and nano composite structures with magneto-electro effects. Fan and Wang (2015) examined nonlinear dynamics of laminated beams reinforced carbon nanotubes with matrix crack under thermal environment. Zenkour (2016) investigated torsional dynamics of carbon nanotubes

*Corresponding author, Ph.D., E-mail: serefda@yahoo.com

http://www.techno-press.org/?journal=amr&subpage=5 ISSN: 2234-0912 (Print), 2234-179X (Online)

embedded in viscoelastic medium. Jena *et al*. (2016) analyzed dynamic behavior of cracked fiber reinforced composite beams. Ghayesh (2018) analyzed forced nonlinear vibration of axially functionally graded micro beams by using coupled stress theory. Akbaş (2015a, 2018b, 2019b) investigated forced vibration analysis of cracked beams. Yaylı (2019) presented free lateral vibration behavior of a functionally graded nanobeam in an elastic matrix with rotationally restrained ends. Draiche *et al*. (2019) presented static analysis of laminated reinforced composite plates based on first-order shear deformation theory by using the Navier method. Waddar *et al*. (2019) investigated buckling and dynamic response of cenosphere reinforced epoxy composite core sandwich beam with sisal fabric/epoxy composite facings under compressive load by experimentally.

As seen from literature survey, the forced vibration studies of FRC beams have not been investigated broadly. In this study, forced vibration responses of a FRC beam are obtained with using Timoshenko beam theory and Ritz method. The governing equations of problem are obtained by using the Lagrange procedure. In the solution of the forced vibration problem, the Newmark average acceleration method is used in the time history. In the numerical results, the effects of fibre orientation angles, the volume fraction and dynamic parameters on the forced vibration response of the FRC beam are presented.

2. Problem formulation

A cantilever FRC beam under a dynamic point load $Q(t)$ at free end is presented in Fig. 1. The geometry parameters of the FRC beam indicate as the length L, the height h and width b. The dynamic point load $Q(t)$ is assumed to be sinusoidal harmonic in time domain as following

$$Q(t) = Q_0 \sin(\overline{\omega} t), \qquad 0 \leq t \ll \infty \tag{1}$$

In Eq. (1), Q_0 and $\overline{\omega}$ indicate the amplitude and the frequency of the dynamic load.

The axial strain (ε_z) and shear strain (γ_{zy}) are given according to the Timoshenko beam theory as follows

$$\varepsilon_z = \frac{\partial u_0}{\partial z} - Y \frac{\partial \emptyset}{\partial z} \tag{2a}$$

$$\gamma_{zy} = \frac{\partial u_0}{\partial y} + \frac{\partial v_0}{\partial z} \tag{2b}$$

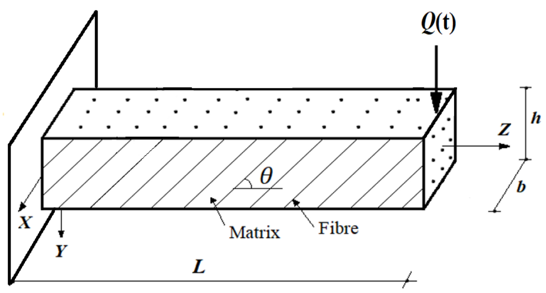

Fig. 1 A cantilever FRC beam under a dynamic point load at free end

where, u_0, v_0 and $\emptyset$ are axial displacement, vertical displacement and rotation, respectively. The constitute relation is presented as follows

$$\begin{Bmatrix} \sigma_z \\ \sigma_{zy} \end{Bmatrix} = \begin{bmatrix} \bar{Q}_{11} & \bar{Q}_{16} \\ \bar{Q}_{16} & \bar{Q}_{66} \end{bmatrix} \begin{Bmatrix} \epsilon_z \\ \gamma_{zy} \end{Bmatrix} \tag{3}$$

where $\overline{Q}_{ij}$ are the transformed components of the reduced constitutive tensor. The transformed components of the reduced constitutive tensor for orthotropic material are as follows

$$\overline{Q}_{11} = Q_{11}l^4 + 2(Q_{12} + 2Q_{66})l^2n^2 + Q_{22}n^4 \tag{4a}$$

$$\overline{Q}_{12} = (Q_{11} + Q_{22} - 4Q_{66})sin^2cos^2 + Q_{12}(l^4 + n^4) \tag{4b}$$

$$\overline{Q}_{16} = (Q_{11} - Q_{12} - 2Q_{66})nl^3 + (Q_{12} - Q_{22} + 2Q_{66})n^3l \tag{4c}$$

$$\overline{Q}_{22} = Q_{11}n^4 + 2(Q_{12} + 2Q_{66})n^2l^2 + Q_{22}l^4 \tag{4d}$$

$$\overline{Q}_{26} = (Q_{11} - Q_{12} - 2Q_{66})n^3l + (Q_{12} - Q_{22} + 2Q_{66})nl^3 \tag{4e}$$

$$\overline{Q}_{66} = (Q_{11} + Q_{22} - 2Q_{12} - 2Q_{66})n^2l^2 + Q_{66}(n^4 + l^4) \tag{4f}$$

where $l = \cos\theta$ and $n = \sin\theta$, θ indicates the fiber orientation angle and the expressions of $\overline{Q}_{ij}$ are as follows

$$Q_{11} = \frac{E_1}{1 - \nu_{12}\nu_{21}}, \qquad Q_{22} = \frac{E_2}{1 - \nu_{12}\nu_{21}} \tag{5a}$$

$$Q_{12} = \frac{\nu_{12}E_2}{1 - \nu_{12}\nu_{21}} = \frac{\nu_{21}E_1}{1 - \nu_{12}\nu_{21}} \tag{5b}$$

$$Q_{21} = \frac{\nu_{12}E_2}{1 - \nu_{12}\nu_{21}} = \frac{\nu_{21}E_1}{1 - \nu_{12}\nu_{21}} \tag{5c}$$

$$Q_{66} = G_{12} \tag{5d}$$

where E_1 is the Young's modulus in the X direction, E_2 is the Young's modulus in the Y direction, ν_{12} and ν_{21} are Poisson's ratios and G_{12} is the shear modulus in XY plane. The gross mechanical properties of the composite materials are calculated by using the following expression (Vinson and Sierakowski 2002)

$$E_1 = E_fV_f + E_m\left(1 - V_f\right), \tag{6a}$$

$$E_2 = E_m\left[\frac{E_f + E_m + \left(E_f - E_m\right)V_f}{E_f + E_m - \left(E_f - E_m\right)V_f}\right] \tag{6b}$$

$$\nu_{12} = \nu_f \ V_f + \nu_m \left(1 - V_f\right), \tag{6c}$$

$$G_{12} = G_m \left[\frac{G_f + G_m + \left(G_f - G_m\right)V_f}{G_f + G_m - \left(G_f - G_m\right)V_f}\right] \tag{6d}$$

$$\rho = \rho_f V_f + \rho_m \left(1 - V_f\right), \tag{6e}$$

where *f* indicates the fibre and *m* indicates the matrix. V_f is the volume fraction of fiber. *E*, *G*, *v* and ρ are the Young's modulus, the shear modulus, Poisson's ratio and mass density, respectively.

The strain energy (U_i), the kinetic energy (*K*), the dissipation function and potential energy of the external loads (U_e) are presented as follows

$$U_i = \frac{1}{2}\int_0^L \left[A_0\left(\frac{\partial u_0}{\partial z}\right)^2 - 2A_1\frac{\partial u_0}{\partial z}\frac{\partial \emptyset}{\partial z} + A_2\left(\frac{\partial \emptyset}{\partial z}\right)^2\right]dZ + \frac{1}{2}\int_0^L K_s B_0\left[\left(\frac{\partial v_0}{\partial z}\right)^2 - 2\frac{\partial v_0}{\partial z}\emptyset + \emptyset^2\right]dZ \tag{7a}$$

$$K = \frac{1}{2}\int_0^L \left(I_0\left(\frac{\partial u_0}{\partial t}\right)^2 - 2I_1\left(\frac{\partial u_0}{\partial t}\right)\left(\frac{\partial \emptyset}{\partial t}\right) + I_2\left(\frac{\partial \emptyset}{\partial t}\right)^2 + I_0\left(\frac{\partial v_0}{\partial t}\right)^2\right)dZ \tag{7b}$$

where

$$(A_0, A_1, A_2) = \int_A \overline{Q}_{11}(1, Y, Y^2)dA\,, \qquad B_0 = \int_A \overline{Q}_{66}dA\,, \qquad (I_0, I_1, I_2) = \int_A \rho(Y)(1, Y, Y^2)dA \tag{8}$$

The Lagrangian functional of the problem is presented as follows;

$$I = K - (U_i + U_e) \tag{9}$$

In the solution of the problem in Ritz method, approximate solution is given as a series of *i* terms of the following form

$$u_0(z,t) = \sum_{i=1}^{\infty} \mathrm{a}_i\,(t)\alpha_i(z) \tag{10a}$$

$$v_0(z,t) = \sum_{i=1}^{\infty} \mathrm{b}_i\,(t)\beta_i(z) \tag{10b}$$

$$\emptyset(z,t) = \sum_{i=1}^{\infty} \mathrm{c}_i\,(t)\gamma_i(z) \tag{10c}$$

where a_i, b_i and c_i are the unknown coefficients, $\alpha_i(z,t)$, $\beta_i(z,t)$, $\gamma_i(z,t)$ are the coordinate functions depend on the boundary conditions over the interval [*0*, *L*]. The coordinate functions for the cantilever beam are given as algebraic polynomials

$$\alpha_i(z) = z^i \tag{11a}$$

$$\beta_i(z) = z^{(i+1)} \tag{11b}$$

$$\gamma_i(z) = z^i \tag{11c}$$

where *i* indicates the number of polynomials involved in the admissible functions.

After substituting Eq. (10) into energy Eq. (7), and then using the Lagrange's equation gives the following equation

$$\frac{\partial I}{\partial q_i} - \frac{\partial}{\partial t}\frac{\partial I}{\partial \dot{q}_i} = 0 \tag{12}$$

where q_i is the unknown coefficients which are a_i, b_i and c_i. After implementing the Lagrange procedure, the motion equation of the problem is obtained as follows

$$[\mathrm{K}]\{\mathrm{q(t)}\} + [\mathrm{M}]\{\ddot{\mathrm{q}}(\mathrm{t})\} = \{\mathrm{F(t)}\} \tag{13}$$

where $[K]$, $[M]$ and $\{\mathrm{F(t)}\}$ are the stiffness matrix, the mass matrix and load vector, respectively. The detail of these expressions are given as follows

$$[K] = \begin{bmatrix} K_{11} & K_{12} & K_{13} \\ K_{21} & K_{22} & K_{23} \\ K_{31} & K_{32} & K_{33} \end{bmatrix} \tag{14}$$

Where

$$\begin{aligned}
&K_{ij}^{11} = \sum_{i=1}^{n}\sum_{j=1}^{n}\int_0^L A_0 \frac{\partial \alpha_i}{\partial z}\frac{\partial \alpha_j}{\partial z}\,dz, \qquad K_{ij}^{12} = 0, \\
&K_{ij}^{13} = -\sum_{i=1}^{n}\sum_{j=1}^{n}\int_0^L A_1 \frac{\partial \alpha_i}{\partial z}\frac{\partial \gamma_j}{\partial z}\,dz, \quad K_{ij}^{21} = 0, \\
&K_{ij}^{11} = \sum_{i=1}^{n}\sum_{j=1}^{n}\int_0^L A_0 \frac{\partial \alpha_i}{\partial z}\frac{\partial \alpha_j}{\partial z}\,dz, \qquad K_{ij}^{22} = \sum_{i=1}^{n}\sum_{j=1}^{n}\int_0^L K_s B_0 \frac{\partial \beta_i}{\partial z}\frac{\partial \beta_j}{\partial z}\,dz, \\
&K_{ij}^{23} = -\sum_{i=1}^{n}\sum_{j=1}^{n}\int_0^L K_s B_0 \frac{\partial \beta_i}{\partial z}\gamma_j\,dz, \quad K_{ij}^{31} = -\sum_{i=1}^{n}\sum_{j=1}^{n}\int_0^L A_1 \frac{\partial \gamma_i}{\partial z}\frac{\partial \alpha_j}{\partial z}\,dz, \\
&K_{ij}^{32} = -\sum_{i=1}^{n}\sum_{j=1}^{n}\int_0^L K_s B_0 \gamma_i \frac{\partial \beta_j}{\partial z}\,dz, \\
&K_{ij}^{33} = \sum_{i=1}^{n}\sum_{j=1}^{n}\int_0^L A_2 \frac{\partial \gamma_i}{\partial z}\frac{\partial \gamma_j}{\partial z} + \sum_{i=1}^{n}\sum_{j=1}^{n}\int_0^L K_s B_0 \gamma_i \gamma_j\,dz,
\end{aligned} \tag{15}$$

$$[M]=\begin{bmatrix}M_{11} & M_{12} & M_{13}\\ M_{21} & M_{22} & M_{23}\\ M_{31} & M_{32} & M_{33}\end{bmatrix} \tag{16}$$

Where

$$\begin{aligned}
&M_{11}=\sum_{i=1}^{n}\sum_{j=1}^{n}\int_{0}^{L}\mathrm{I}_0\,\alpha_i\alpha_j\mathrm{dz}, \qquad M_{12}=0\\
&M_{13}=-\sum_{i=1}^{n}\sum_{j=1}^{n}\int_{0}^{L}\mathrm{I}_1\,\alpha_i\gamma_j\mathrm{dz}, \qquad M_{21}=0,\\
&M_{22}=\sum_{i=1}^{n}\sum_{j=1}^{n}\int_{0}^{L}\mathrm{I}_0\,\beta_i\beta_j\mathrm{dz}, \qquad M_{23}=M_{32}=0\\
&M_{31}=-\sum_{i=1}^{n}\sum_{j=1}^{n}\int_{0}^{L}\mathrm{I}_1\,\gamma_i\alpha_j\mathrm{dz}\\
&M_{33}=\sum_{i=1}^{n}\sum_{j=1}^{n}\int_{0}^{L}\mathrm{I}_2\,\gamma_i\gamma_j\mathrm{dz}
\end{aligned} \tag{17}$$

$$\{\mathrm{F(t)}\}=Q\beta_j \tag{18}$$

The governing equation of motions Eq. (13) is solved numerically by using implicit Newmark average acceleration method in the time domain.

3. Numerical results

In this section, dynamical displacements of the FRC cantilever beam are presented and discussed. In the numerical examples, the materials of the beams are selected as made of graphite fibre-reinforced polyamide composite and its material parameters are as follows (Krawczuk *et al*. 1997); E_m = 2.756 GPa, E_f = 275.6 GPa, G_m = 1.036 GPa, G_f = 114.8 GPa, ν_m = 0.33, ν_f = 0.2, ρ_m = 1600 kg/m^3, ρ_f = 1900 kg/m^3. The geometry properties of the beam are selected as $b = 0.1$ m, h = 0.1 m and L = 1.2 m. In the numerical results, number of the series term is taken as 10. The amplitude of the dynamic load is selected as Q_0 = 1 kN.

In order to investigate the effects of the fiber orientation angles (θ), the lateral dynamical displacements of the FRC beams are presented for different values of θ in Figs. 2 and 3 in the time history. In these figures, the maximum dynamical displacements (v_{max}) are calculated at the free end of the beam. In Fig. 2, the time history of FRC cantilever beam is presented in the dynamical displacements for $V_f = 0.3$, $\overline{\omega} = 10\ rd/s$. In Fig. 3, the relationship between of the maximum displacements and the frequency of the dynamic load ($\overline{w}$) of FRC cantilever beam is presented for different values the fiber orientation angles for $V_f = 0.3$ for t = 0.5 s.

It is seen from Figs. 2 and 3 that increasing the fiber orientation angles, the dynamical lateral displacements of the FRC beam increase considerably. The bending rigidity decreases with increasing the fiber orientation angles according to Eq. (4), so the displacements increase. Also, as seen from Fig. 3, the displacements increase and the resonance frequencies decrease with increasing in the fiber orientation angles. In Fig. 3, the resonance frequencies can be observed in the asymptote lines. The fiber orientation angles play important role on the dynamic responses of FRC beams.

In Figs. 4 and 5, effects of the volume fraction of fiber (V_f) on the dynamic responses of FRC cantilever beam are displayed for different values of V_f. In Fig. 4, the time history of FRC cantilever beam is presented in the dynamical displacements for $\theta = 30^{\circ}$, $\overline{\omega} = 10\, rd/s$. In Fig. 5, the relationship between of the maximum displacements and the frequency of the dynamic load ($\overline{w}$) of FRC cantilever beam is presented for different values the V_f for $\theta = 30^{\circ}$ for $t = 0.5$ s.

It is observed from Fig. 4 that increasing volume fraction of fiber yields to decrease dynamical displacements significantly. The reason of this situation that with increasing the volume fraction of fiber V_f, the rigidity of the FRC beam increases, so displacements decreases naturally. In addition,

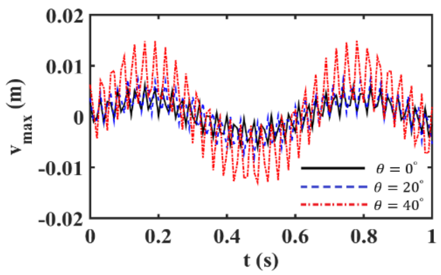

Fig. 2 Time history of the FRC cantilever beam for different values the fiber orientation angles

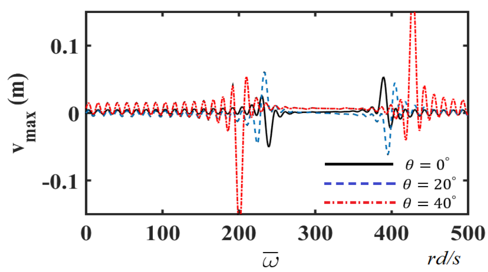

Fig. 3 The relationship between of the maximum displacements and the frequency of the dynamic load ($\overline{w}$) of FRC cantilever beam for different values the fiber orientation angles

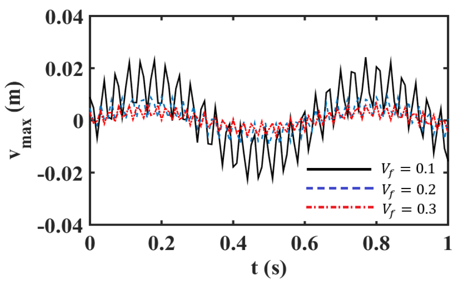

Fig. 4 Time history of the FRC cantilever beam for different values the volume fraction of fiber (V_f)

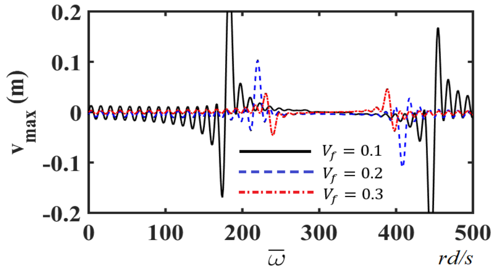

Fig. 5 The relationship between of the maximum displacements and the frequency of the dynamic load ($\overline{w}$) of FRC cantilever beam for different values the volume fraction of fiber (V_f)

the resonance frequencies of the FRC beam increase with increasing of the volume fraction of fiber. Because of increasing the volume fraction of fiber, the FRC beam gets more strength and so, the resonance frequencies increase. It shows that the volume fraction of fiber is very effective on the dynamic responses of FRC beams.

4. Conclusions

Dynamic responses of FRC cantilever beam under a dynamically harmonic load are studied in the framework of the Timoshenko beam theory. Ritz method and Newmark integration method are exploited to solve the equation of motion incrementally. Effects of fibre orientation angles, the volume fraction and dynamic parameters on the Dynamically displacements of the FRC beam investigated. The most findings of this article can be summarized as:

The fiber orientation angles has significant effects on dynamic response and amplitude of oscillation. The displacement of FRC beam is increased dramatically as the fiber orientation angle increased. The resonance frequencies of the FRC beam increase with increasing of the volume fraction of fiber significantly. The results show that the dynamical behavior of FRC beams change dramatically with the material properties.

References

Akbaş, Ş.D. (2014a), "Wave propagation analysis of edge cracked circular beams under impact force", *PloS one*, **9**(6), e100496. https://doi.org/10.1371/journal.pone.0100496

Akbaş, Ş.D. (2014b), "Free vibration of axially functionally graded beams in thermal environment", *Int. J. Eng. Appl. Sci.*, **6**(3), 37-51. https://doi.org/10.24107/ijeas.251224

Akbaş, Ş.D. (2014c), "Wave propagation analysis of edge cracked beams resting on elastic foundation", *Int. J. Eng. Appl. Sci.*, **6**(1), 40-52. https://doi.org/10.24107/ijeas.251218

Akbaş, Ş.D. (2015a), "Free Vibration Analysis of Edge Cracked Functionally Graded Beams Resting on Winkler-Pasternak Foundation", *Int. J. Eng. Appl. Sci.*, **7**(3), 1-15. https://doi.org/10.24107/ijeas.251252

Akbaş, Ş.D. (2015b), "Free vibration and bending of functionally graded beams resting on elastic foundation", *Res. Eng. Struct. Mater.*, **1**(1), 25-37. http://dx.doi.org/10.17515/resm2015.03st0107

Akbaş, Ş.D. (2018a), "Investigation on free and forced vibration of a bi-material composite beam", *J. Polytechnic-Politeknik Dergisi*, **21**(1), 65-73. http://dx.doi.org/10.2339/politeknik.386841

Akbaş, Ş.D. (2018b), "Forced vibration analysis of cracked nanobeams", *J. Brazil. Soc. Mech. Sci. Eng.*, **40**(8), 392. https://doi.org/10.1007/s40430-018-1315-1

Akbaş, Ş.D. (2018c), "Investigation of static and vibration behaviors of a functionally graded orthotropic beam", Balıkesir Üniversitesi Fen Bilimleri Enstitüsü Dergisi, 1-14. https://doi.org/10.25092/baunfbed.343227

Akbaş, Ş.D. (2019a), "Forced vibration analysis of functionally graded sandwich deep beams", *Coupl. Syst. Mech., Int. J.*, **8**(3), 259-271. http://dx.doi.org/10.12989/csm.2019.8.3.259

Akbaş, Ş.D. (2019b), "Axially Forced Vibration Analysis of Cracked a Nanorod", *J. Computat. Appl. Mech.*, **50**(1), 63-68. http://dx.doi.org/10.22059/jcamech.2019.281285.392

Akbaş, Ş.D. (2019c), "Longitudinal Forced Vibration Analysis of Porous A Nanorod", *J. Eng. Sci. Des.*, **7**(4), 736-743. http://dx.doi.org/10.21923/jesd.553328

Akbaş, Ş.D. (2021), "Forced Vibration Responses of Axially Functionally Graded Beams by using Ritz Method", *J. Appl. Computat. Mech.*, **7**(1), 109-115. http://dx.doi.org/10.22055/JACM.2020.34865.2491

DeValve, C. and Pitchumani, R. (2014), "Analysis of vibration damping in a rotating composite beam with embedded carbon nanotubes", *Compos. Struct.*, **110**, 289-296. https://doi.org/10.1016/j.compstruct.2013.12.007

Draiche, K., Bousahla, A.A., Tounsi, A., Alwabli, A.S., Tounsi, A. and Mahmoud, S.R. (2019), "Static analysis of laminated reinforced composite plates using a simple first-order shear deformation theory", *Comput. Concrete, Int. J.*, **24**(4), 369-378. https://doi.org/10.12989/cac.2019.24.4.369

Ebrahimi, F., Barati, M.R. and Dabbagh, A. (2016), "Wave dispersion characteristics of axially loaded magneto-electro-elastic nanobeams", *Appl. Phys. A*, **122**(11), 949.

Ebrahimi, F. and Barati, M.R. (2017), "Dynamic modeling of magneto-electrically actuated compositionally graded nanosize plates lying on elastic foundation", *Arab. J. Sci. Eng.*, **42**(5), 1977-1997.

Fan, Y. and Wang, H. (2015), "Nonlinear vibration of matrix cracked laminated beams containing carbon nanotube reinforced composite layers in thermal environments", *Compos. Struct.*, **124**, 35-43. https://doi.org/10.1016/j.compstruct.2014.12.050

Ghayesh, M.H. (2018), "Mechanics of tapered AFG shear-deformable microbeams", *Microsyst. Technologies*, **24**(4), 1743-1754. https://doi.org/10.1007/s00542-018-3764-y

Jena, P.C., Parhi, D.R. and Pohit, G. (2016), "Dynamic Study of Composite Cracked Beam by Changing the Angle of Bidirectional Fibres", *Iran. J. Sci. Technol., Transactions A: Science*, **40**(1), 27-37. https://doi.org/10.1007/s40995-016-0006-y

Krawczuk, M., Ostachowicz, W. and Zak, A. (1997), "Modal analysis of cracked, unidirectional composite beam", *Compos. Part B: Eng.*, **28**(5-6), 641-650. https://doi.org/10.1016/S1359-8368(97)82238-X

Mohanty, S.C., Dash, R.R. and Rout, T. (2015), "Vibration and dynamic stability of pre-twisted thick cantilever beam made of functionally graded material", *Int. J. Struct. Stabil. Dyn.*, **15**(4), 1450058. https://doi.org/10.1142/S0219455414500588

Palanivel, S. (2006), "Dynamic analysis of laminated composite beams using higher order theories and finite elements", *Compos. Struct.*, **73**(3), 342-353. https://doi.org/10.1016/j.compstruct.2005.02.002

Pour, H.R., Vossough, H., Heydari, M.M., Beygipoor, G. and Azimzadeh, A. (2015), "Nonlinear vibration analysis of a nonlocal sinusoidal shear deformation carbon nanotube using differential quadrature method", *Struct. Eng. Mech., Int. J.*, **54**(6), 1061-1073. https://doi.org/10.12989/sem.2015.54.6.1061

Tornabene, F., Fantuzzi, N., Viola, E. and Reddy, J.N. (2014), "Winkler–Pasternak foundation effect on the static and dynamic analyses of laminated doubly-curved and degenerate shells and panels", *Compos. Part B: Eng.*, **57**, 269-296. https://doi.org/10.1016/j.compositesb.2013.06.020

Vinson, J.R. and Sierakowski, R.L. (2002), *Behaviour of Structures Composed of Composite Materials*, Kluwer Academic Publishers, ISBN 978-140-2009-04-4, Netherlands. https://doi.org/10.1007/0-306-48414-5

Fan, Y. and Wang, H. (2017), "The effects of matrix cracks on the nonlinear vibration characteristics of shear deformable laminated beams containing carbon nanotube reinforced composite layers", *Int. J. Mech. Sci.*, **124**, 216-228. https://doi.org/10.1016/j.ijmecsci.2017.03.016

Waddar, S., Pitchaimani, J., Doddamani, M. and Barbero, E. (2019), "Buckling and vibration behaviour of syntactic foam core sandwich beam with natural fiber composite facings under axial compressive loads", *Compos. Part B: Eng.*, **175**, 107133. https://doi.org/10.1016/j.compositesb.2019.107133

Yayli, M.Ö. (2019), "Free vibration analysis of a rotationally restrained (FG) nanotube", *Microsyst.*

Technologies, **25**(10), 3723-3734. https://doi.org/10.1007/s00542-019-04307-4
Zenkour, A.M. (2016), "Torsional Dynamic Response of a Carbon Nanotube Embedded in Visco-Pasternak's Medium", *Mathe. Model. Anal.*, **21**(6), 852-868. https://doi.org/10.3846/13926292.2016.1248510

CC